Electronic structure and magnetism in sodium nickelate: Density-functional and model studies

H. Meskine and S. Satpathy
Department of Physics & Astronomy, University of Missouri, Columbia, Missouri 65211, USA
(Received 15 August 2005; published 15 December 2005)

The electronic structure and magnetism in $NaNiO_2$ are studied from density-functional calculations and by solving model Hamiltonians, suggested from the density-functional results, to understand the magnetic exchange. The density-functional calculations within the LSDA approximation yield a layered antiferromagnetic solution with ferro-orbital ordering of the Ni(d) orbitals arising from the Jahn-Teller distortion around the Ni^{3+} ion in agreement with the orbital ordering inferred from neutron diffraction. The weak ferromagnetic interaction within the layer ($J_F \approx 1$ meV) is caused by the 90° Ni-O-Ni exchange following the Goodenough-Kanamori-Anderson rules, while the weaker antiferromagnetic interaction between the layers ($J_{AF} \approx -0.1$ meV) is mediated via a long Ni-O-Na-O-Ni superexchange path. In order to shed light on the differences between $NaNiO_2$ and $LiNiO_2$, which show very different magnetic behaviors in spite of the similarity of their crystal structures, we examine the effect of the coupling of the alkali atom (Na) motion to the electronic degrees of freedom on the interlayer exchange J_{AF}. A model Hamiltonian is proposed and solved by exact diagonalization and by using the variational Lang-Firsov method. We find that reducing the mass by going from Na to Li does reduce the strength of the magnetic exchange, but only by a small amount, so that the difference in mass alone cannot describe the differences in magnetic behavior between the two compounds. It is suggested that other electronic effects such as differences in orbital ordering could be responsible for the difference in magnetism between $NaNiO_2$ and $LiNiO_2$.

DOI: 10.1103/PhysRevB.72.224423 PACS number(s): 75.10.−b, 71.20.Dg, 63.20.Dj

I. INTRODUCTION

It is a puzzle as to why the two compounds $NaNiO_2$ and $LiNiO_2$, in spite of having very similar crystal structures, show very different magnetic properties. The former is a type-*A* antiferromagnet (ferromagnetic layers coupled antiferromagnetically; Fig. 1), while the latter shows no long-range magnetic order. Experiments[1] on $NaNiO_2$ have revealed that the antiferromagnetic exchange interaction J_{AF} between the layers is considerably weaker than the ferromagnetic exchange J_F within the layer, $J_F \approx 1$ meV and $J_{AF} \approx -0.1$ meV. It is conceivable that the superexchange path between the layers being Ni-O-Na-O-Ni, replacing Na by Li weakens the interplanar superexchange sufficiently so as to destroy the magnetism altogether, since the two-dimensional (2D) magnetism becomes untenable by virtue of the Mermin-Wagner theorem.[2]

The reduction of the interplanar coupling could come either through differences in the electronic parameters such as the hopping parameters and charge-transfer energy or simply through the mass difference of the intervening alkali atom, which is quite large between Na and Li. In view of the fact that isotope substitution has been known to alter the magnetic interactions, changing the magnetic transition temperature T_c in a variety of compounds such as Fe_3O_4 (Ref. 3) and the manganites,[4–6] it is important to examine the effect of the alkali mass.

In this paper, we focus on the compound $NaNiO_2$. Starting with the density-functional band structure, we study the mechanism of the magnetic interaction as well as the effect of the sodium mass on it. We study this by proposing a model for the superexchange and solving it by a variational Lang-Firsov approach as well as by exact diagonalization and the fourth-order perturbation theory. From our model, we explain the mechanism of the exchange interactions for $NaNiO_2$, ferromagnetic within the layer and antiferromagnetic between the layers. However, we find that although there is some effect of the alkali mass on the magnetic interactions, it is not enough to describe the suppression of magnetism in $LiNiO_2$. It is suggested that differences in the electronic structure such as orbital ordering or simply the magnitudes of the Hamiltonian parameters could further reduce J_{AF}, enough to suppress the 2D magnetism in $LiNiO_2$.

II. ELECTRONIC STRUCTURE OF $NaNiO_2$

We begin by discussing the *ab initio* electronic structure calculations based on the density functional theory (DFT). At high temperature, $NaNiO_2$ has the simple hexagonal crystal structure (space group $R\bar{3}m$, no. 166) shown in Fig. 1, and undergoes a structural transition to a lower-symmetry monoclinic structure with the paramagnetic space group $C2/m$ (no. 12) at about 500 K.[1] This latter structure is layered and may be viewed as an arrangement of slightly elongated NiO_6 octahedra separated by Na sheets. The NiO_6 octahedra in this material are edge sharing such that the Ni ions form a triangular lattice. There are two types of oxygen atoms due to the strong Jahn-Teller (JT) distortion of the NiO_6 octahedra, giving rise to two different Ni-O bond lengths: four short bonds of approximately 1.91 Å, and two long ones of 2.14 Å. The lattice parameters are taken from Ref. 1. The magnetic structure of this material is antiferromagnetic (AF) of type *A* with a Neel temperature of $T_N \approx 20$K.[7]

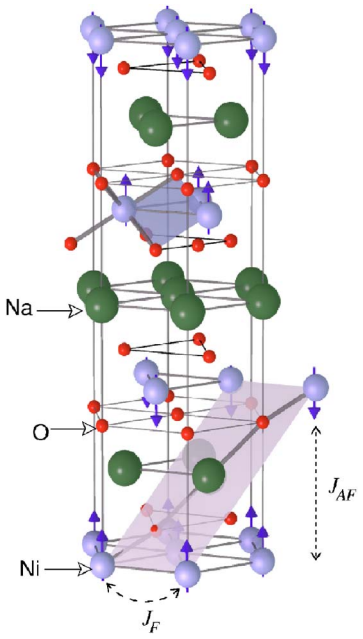

FIG. 1. (Color online) Crystal structure of $NaNiO_2$ at high temperature (Ref. 7). The low-temperature structure is obtained by distorting the NiO_6 octahedra along the long Ni-O-Na-O-Ni bond shown in the figure. The magnetic ordering is antiferromagnetic type A and the two types of Ni-Ni exchange interactions J_F and J_{AF} are shown. The shaded plane is the plane of the charge density plot in Fig. 4. The shaded square in the upper portion of the figure shows the Ni-O-Ni-O plaquette for the 90° exchange as discussed in the text.

The *ab initio* electronic structure calculations were performed for the low-temperature structure using the local spin-density approximation (LSDA) to density functional theory (DFT). The DFT calculation is discussed in more details in Ref. 8, so in this paper we shall only state the main results. The self-consistent tight-binding linear muffin-tin orbitals (TB LMTO) method was used.[9,10] In addition we made use of the LSDA+U correction[11] to better account for the correlation effects. The on-site Coulomb energy of $U=5$ eV for the Ni(d) orbitals was used. In the magnetic calculation, the symmetry is not reduced further and the magnetic unit cell is also monoclinic with space group $C2/m$ with two formula units per unit cell. The calculations were scalar relativistic and the von Barth-Hedin[12] exchange-correlation potential was used.

Within the LMTO atomic sphere approximation (LMTO-ASA), the AF-A structure was found to be the ground state, lower in energy than both the ferromagnetic and paramagnetic configurations. It was found that the Ni ion is in a low spin state with the nominal occupations $t_{2g}^6 e_g^1$ and a magnetic moment $\mu \approx 0.5\ \mu_B$/Ni ion. The magnetic moment is significantly reduced from the expected Hund's rule value of $\mu=1\ \mu_B$/Ni due to the strong hybridization of the Ni(d) and O(p) orbitals.

The band structure is shown in Fig. 2. The bands are consistent with a low-spin state, with the t_{2g} states being completely occupied while the e_g states are only 1/2-filled ($t_{2g}^6 e_g^1$). The t_{2g} and e_g bands are split by a strong crystal field,

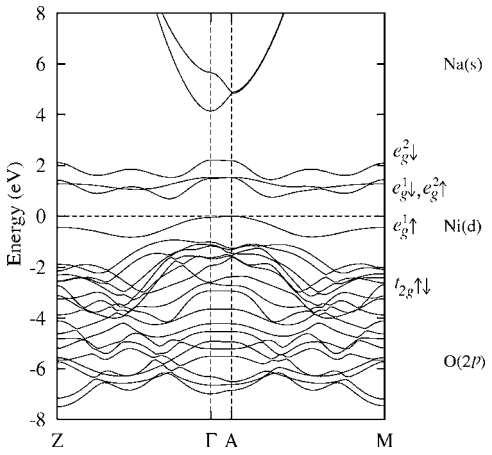

FIG. 2. Density-functional electron bands for the antiferromagnetic $NaNiO_2$ obtained from the LSDA+U calculations. The low-temperature crystal structure with two formula units in the unit cell was used in the calculation. The e_g bands are split near the Fermi level due to the Jahn-Teller and exchange interactions. The LSDA calculation without the Coulomb U correction produces a similar band structure, except that the lowest e_g band ($e_g^1\uparrow$) is not completely detached from the rest of the e_g bands, resulting in a metallic band structure.

while the $e_g^\uparrow$ and $e_g^\downarrow$ are split by the exchange coupling with a strength $\Delta_{ex} \approx 0.5$ eV. The Ni(d) occupation being $t_{2g}^6 e_g^1$, the atom is JT active and the degeneracy of the e_g levels is then lifted, with a JT splitting $\Delta_{JT} \approx 0.6$ eV. The one-electron densities of states are shown in Fig. 3.

We have also computed the electronic charge density for an energy range which includes only the valence e_g band. In a frame of reference where the z axis points along the long Ni-O bond, we found this band to be of $3z^2-r^2$ character. The charge-density contours are plotted in Fig. 4, which clearly shows the "ferro-orbital ordering," where all the $3z^2-r^2$ orbitals on all Ni atoms in the structure are oriented along the same direction, towards the elongated Ni-O bond which lies on the Ni-O-Na-O-Ni superexchange path as in-

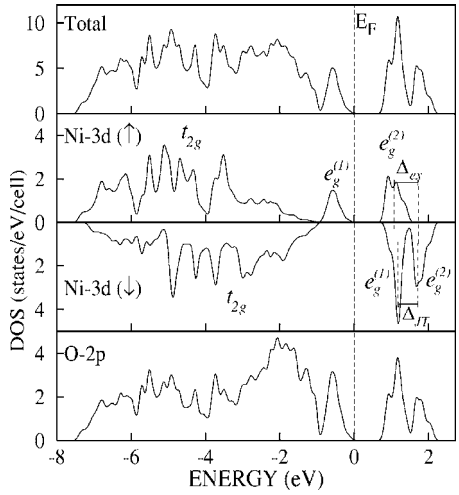

FIG. 3. One-electron densities of states for antiferromagnetic $NaNiO_2$.

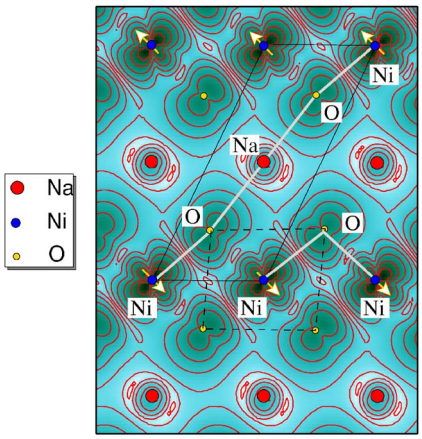

FIG. 4. (Color online) Charge-density contours for the occupied Ni(e_g) bands obtained from the local spin-density approximation and plotted on the shaded plane shown in Fig. 1. The plane contains both the Ni-O-Na-O-Ni and the 90° Ni-O-Ni superexchange paths. The dashed-line rectangle indicates the Jahn-Teller distorted NiO_6 octahedron. All Ni(d) orbitals in the crystal are oriented along the same direction indicating the so-called ferrodistorsive orbital ordering, inferred from the neutron scattering experiments (Refs. 13 and 14).

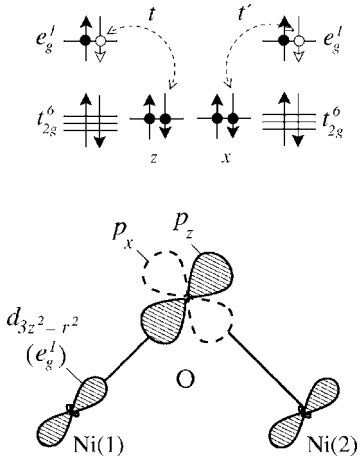

FIG. 5. Model for the 90° Ni-O-Ni exchange interaction within the layer. Open arrows represent the holes. Double-arrowed, dashed lines indicate virtual processes with the hopping of the e_g^1 electrons from the neighboring transition-metal atoms to the oxygen atom giving rise to the ferromagnetic interaction.

dicated in the figure. Electronic structure calculations for the high-temperature structure, which has undistorted NiO_6 octahedra, were also performed and no orbital ordering was found for this structure.

III. MAGNETISM IN $NaNiO_2$

A. Intralayer exchange

The ferromagnetic exchange interaction within the plane is mediated via the oxygen atom forming the 90° Ni-O-Ni bond, which is weakly ferromagnetic according to the celebrated Goodenough-Kanamori-Anderson rules. The rule states that the 90° exchange between filled orbitals is ferromagnetic and relatively weak.[15,16]

To illustrate this for the present compound, we adopt a simple model shown in Fig. 5, retaining only the z^2 orbital as the active orbital for electron transfer on the two transition metals, consistent with the orbital ordering shown in Fig. 4. The Ni t_{2g} orbitals are fully occupied. There are actually two 90° Ni-O-Ni paths forming a square plaquette as shown in Fig. 4, so that, considering the two paths to be independent, the exchange will be twice the magnitude calculated for a single Ni-O-Ni path.

We assume that if two e_g electrons are present on the transition metal atom, they both will occupy the $z^2\uparrow\downarrow$ orbitals, which is favored by the Jahn-Teller energy gain. The alternative configuration of $z^2\uparrow$, $x^2-y^2\uparrow$ is considered to have a higher energy, because although favored by the Hund's rule, there is no JT energy gain for this state, which is important since two electronic states are occupied. With this reasoning we omit the x^2-y^2 orbital altogether in our model.

The magnetic interactions are best described in terms of the holes. With the oxygen shell full and the Ni z^2 orbitals occupied by one electron each, we have just two holes present in the system. The Hamiltonian then reads

$$H = \sum_{\sigma} t(d_{1\sigma}^{\dagger}c_{z\sigma} + \text{h.c.}) + t'(d_{2\sigma}^{\dagger}c_{x\sigma} + \text{h.c.}) + \Delta \sum_{p=x,z} \sum_{\sigma} c_{p\sigma}^{\dagger}c_{p\sigma} + \sum_{p=x,z} U_p n_{p\uparrow}n_{p\downarrow} - J_H(n_{x\uparrow}n_{z\uparrow} + n_{x\downarrow}n_{z\downarrow}). \quad (1)$$

Here, the creation operator for a hole of spin σ on the oxygen in the $p=x$ or z orbital is denoted by $c_{p\sigma}^{\dagger}$, while the same for the two Ni sites are denoted by $d_{1\sigma}^{\dagger}$ and $d_{2\sigma}^{\dagger}$, respectively. The Coulomb energy and the Hund's exchange coupling on the oxygen site are denoted by U_p and J_H, while Δ is the charge transfer energy of the hole from the nickel to the oxygen site. The holes hop between Ni(1) and O(p_z) and between Ni(2) and O(p_x) orbitals, with the two hopping matrix elements being t and t', respectively. According to Harrison's tight-binding parametrization,[18] we have $t' \approx -t/2 = -V_{pd\sigma}/2$.

It is quite simple now to obtain the energies of the AF and ferromagnetic (FM) states of the two holes and take the difference to yield the exchange energy

$$J = E_{\uparrow\downarrow} - E_{\uparrow\uparrow}. \quad (2)$$

Consider the FM case with the parallel alignment of the two e_g electrons. The two spin-down holes are distributed among the four spin-up states of oxygen and nickel. Of the total six configurations ($^4C_2$), there are only four that are relevant for the ground state, viz., $\{|\uparrow 00\uparrow\rangle, |0\uparrow 0\uparrow\rangle, |\uparrow 0\uparrow 0\rangle, |0\uparrow\uparrow 0\rangle\}$. The remaining $|\uparrow\uparrow 00\rangle$ and $|00\uparrow\uparrow\rangle\}$ configurations don't mix, because there is no possibility of hole transfer between the two Ni atoms. The arrows here refer to the spin of the hole, where the first and the fourth labels in each configuration represent Ni1 and Ni2, while the second and the third labels represent p_z and p_x orbitals on the oxygen. Similarly, we only have the four relevant configurations $\{|\uparrow 00\downarrow\rangle, |0\uparrow 0\downarrow\rangle, |\uparrow 0\downarrow 0\rangle, |0\uparrow\downarrow 0\rangle\}$ for the AF case.

Both the FM and AF Hamiltonians are then written as

$$H = \begin{pmatrix} 0 & t & t' & 0 \\ t & \Delta & 0 & t' \\ t' & 0 & \Delta & t \\ 0 & t' & t & \Delta' \end{pmatrix}, \tag{3}$$

where $\Delta' = 2\Delta + U_p - J_H$ for the FM case and $\Delta' = 2\Delta + U_p$ for the AF case. It is obvious from the structure of the Hamiltonian why the FM state will have the lower energy. The only difference between the two Hamiltonians is the on-site energy Δ', which is lower in the FM case and hence a larger gain of the hybridization energy by configuration mixing.

Quantitatively, the ground-state energies for the FM and AF configurations are computed using the standard fourth-order nondegenerate perturbation theory[17] and taking the off-diagonal part of the Hamiltonian as the perturbation. Applying this to the Hamiltonians Eq. (3), we obtain the intralayer exchange (denoted commonly by J_F for this compound) to be

$$J_F = 2 \times \frac{V_{pd\sigma}^4}{\Delta^2}\left(\frac{1}{U_p + 2\Delta - J_H} - \frac{1}{U_p + 2\Delta}\right), \tag{4}$$

where the factor of 2 comes from the fact that there are two 90° Ni-O-Ni paths on the square plaquette. The result is consistent with the expression given by Mostovoy and Khomskii[19] and is weakly ferromagnetic in agreement with one of the Goodenough-Kanamori-Anderson rules, which states that: "A 90°-exchange between half-filled orbitals is ferromagnetic and weak."[16]

The basic physical mechanism of the ferromagnetic coupling is simple. For the FM alignment of the Ni spins, the two-hole state on oxygen has the same spins, whose energy is lower by J_H (Hund's energy on the oxygen site) as compared to the energy of the two-hole state with opposite spins. The latter is relevant for virtual hopping in the case of the AF alignment of the Ni spins. Virtual hopping therefore produces a larger gain of energy for the FM case than for the AF case. It is this difference that leads to the FM interaction as seen explicitly from the perturbation-theory result of Eq. (4). Within our model, the magnetic exchange would be zero if there was no Hund's energy on the oxygen site.

It is clear from Eq. (4) that the interaction is always ferromagnetic, irrespective of the Hamiltonian parameters. However, as usual, the strength of the interaction is obviously quite sensitive to the magnitude of the parameters. Taking typical parameters: $V_{pd\sigma}=1$ eV, $\Delta=4$ eV, $U_p=5$ eV, and $J_H=1$ eV, we find the value for $J_F \approx 10$ K, which is of the same order of magnitude as the measured value of 13 K.[1]

B. Interlayer exchange

We now turn to the interlayer exchange coupling, which is experimentally antiferromagnetic and in view of it, is denoted by the symbol J_{AF}. The superexchange path is the Ni-O-Na-O-Ni path as shown in Fig. 1 and also in Fig. 4. Similar paths that connect the Ni atoms on the adjacent layers but with a 90° bend at the Na atom (see Fig. 4) will have less contribution to exchange, because of the type of orbital ordering of the half-filled Ni(e_g) orbitals. Unoccupied Ni(e_g) orbitals have higher energy and will contribute much less to the exchange because of the larger energy denominator and are omitted in the model Hamiltonian like in the previous section.

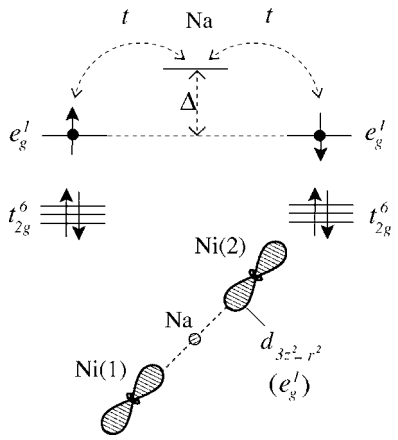

FIG. 6. A three-site model for the magnetic exchange between the layers. The virtual hopping between nickel and sodium occurs via the intermediate oxygen atom, which is replaced in the model by an effective direct hopping between the nickel and the oxygen sites.

We examine the magnetic exchange based on a simple three site model schematically shown in Fig. 6, where the electrons hop between the two Ni(e_g) orbitals located on the adjacent layers via the intermediate Na(s). In reality the Ni-Na hopping takes place via the intermediate O(p) orbitals, but for the sake of simplicity we have considered only the *effective* Ni-Na hopping t.

It is more convenient for the interlayer case to write the Hamiltonian for the electrons rather than for the holes. There are two electrons in the system and, again, our goal is to calculate the AF-FM energy difference to determine the magnetic exchange. The Hamiltonian reads

$$H_{el} = \sum_{\langle i,j\rangle\sigma} t_{ij}(c_{i\sigma}^\dagger c_{j\sigma} + \text{h.c.}) + \sum_i \varepsilon_i n_i + U_i n_{i\uparrow} n_{i\downarrow}, \tag{5}$$

where $c_{i\sigma}^\dagger$ denotes the creation operators for the electrons, t is the effective Ni-Na hopping, ε_i is the on-site energy at site i, where $i=1,2,3$ are, respectively, Ni(1), Na, and Ni(2) atoms, and U_i is the on-site Coulomb interaction on the Ni ($U_1=U_3=U_d$) and Na sites ($U_2=U_s$). Note that for simplicity, we do not include in the model Hamiltonian the Jahn-Teller split e_g^2 orbital (x^2-y^2) because of its higher energy. In the present section, the hopping between Ni and Na is fixed $t_{ij}=t$; however, it will be dependent on the atom positions when we include the electron-phonon coupling in a latter section.

The Hamiltonian for the FM state below is given in the basis set: $\{|110\rangle, |101\rangle, |011\rangle\}$, in that order, while the basis set used for the AF state is: $\{|100;001\rangle, |100;010\rangle, |100;100\rangle, |010;001\rangle, |010;010\rangle, |010;100\rangle, |001;001\rangle, |001;010\rangle, |001;100\rangle\}$, where the first three numbers in each configuration correspond to the occupations of the spin $\uparrow$; orbitals on the Ni(1), Na, and Ni(2) atoms, respectively, while the remaining three numbers correspond to the occupation of the corresponding spin $\downarrow$ orbitals.

With these basis sets, the Hamiltonians read

$$H_{\uparrow\uparrow} = \begin{pmatrix} \Delta & t & 0 \\ t & 0 & t \\ 0 & t & \Delta \end{pmatrix}$$

and

$$H_{\uparrow\downarrow} = \begin{pmatrix} 0 & t & 0 & t & 0 & 0 & 0 & 0 & 0 \\ t & \Delta & t & 0 & t & 0 & 0 & 0 & 0 \\ 0 & t & U_d & 0 & 0 & t & 0 & 0 & 0 \\ t & 0 & 0 & \Delta & t & 0 & t & 0 & 0 \\ 0 & t & 0 & t & U_s + 2\Delta & t & 0 & t & 0 \\ 0 & 0 & t & 0 & t & \Delta & 0 & 0 & t \\ 0 & 0 & 0 & t & 0 & 0 & U_d & t & 0 \\ 0 & 0 & 0 & 0 & t & 0 & t & \Delta & t \\ 0 & 0 & 0 & 0 & 0 & t & 0 & t & 0 \end{pmatrix}. \quad (6)$$

The Ni-Na charge-transfer energy cost Δ is given by

$$\Delta = \varepsilon_s - \varepsilon_d + \frac{1}{2}\Delta_{JT}, \quad (7)$$

where ε_s and ε_d are the Na and Ni on-site energies, respectively, and Δ_{JT} is the Jahn-Teller splitting between the two e_g orbitals as seen in Fig. 3, so that half of it is the JT energy gain for the electron.

First of all, we can conclude from the structure of the two Hamiltonians that the ground-state energy for the parallel configuration is higher than that of the antiparallel configuration, for the simple reason that $H_{\uparrow;\uparrow}$ forms a diagonal subblock of $H_{\uparrow;\downarrow}$, so that the variational principle dictates the latter to have the lower ground-state energy, leading thus to an antiferromagnetic exchange.

For a quantitative result, we need to obtain the ground-state energies correct to the fourth order in the perturbation theory. For the FM case, the exact ground-state energy is given by

$$E_{\uparrow\uparrow} = (\Delta - \sqrt{\Delta^2 + 8t^2})/2. \quad (8)$$

For the AF case, the exact expression for the ground-state energy is rather complicated and also the fourth-order (degenerate) perturbation theory is quite involved, unless the degeneracy is removed in a low order in the perturbation,[20] which is not the case here. Often in the literature, nondegenerate perturbation theory is applied erroneously in such cases, leading to a wrong prediction of the prefactor of the fourth-order term.

In the present case, fortunately, the symmetry present in $H_{\uparrow;\downarrow}$ allows us to compute the ground-state energy $E_{\uparrow;\downarrow}$ in the following manner. Taking the form of the ground-state eigenfunction as $|1,\alpha,\beta,\alpha,\gamma,\alpha,\beta,\alpha,1\rangle$ from symmetry and operating $H_{\uparrow;\downarrow}$ [Eq. (6)] on it, we find that the eigenvalue λ satisfies the following transcendental equation:

$$\lambda^{-1} = (2U_d + U_s + 2\Delta - 3\lambda)(U_d - \lambda)^{-1}(U_s + 2\Delta - \lambda)^{-1} - (\Delta - \lambda)/(2t^2), \quad (9)$$

which we solve by an iterative method by starting with the initial guess $\lambda^{(0)}=0$, which is the unperturbed energy, and iterating the expression (9) until convergence is achieved to the fourth order in the perturbation t. The result is

$$E_{\uparrow\downarrow} = -\frac{2t^2}{\Delta} + \frac{4t^4}{\Delta^3} - \frac{4t^4}{\Delta^2}\left(\frac{1}{U_d} + \frac{2}{U_s + 2\Delta}\right) + O(t^6). \quad (10)$$

Taking the energy difference between the FM and the AF configurations from Eqs. (8) and (10), we get the interlayer exchange to be[21]

$$J_{AF} = -\frac{4t^4}{\Delta^2}\left(\frac{1}{U_d} + \frac{2}{U_s + 2\Delta}\right). \quad (11)$$

It is clear that the interaction is always antiferromagnetic, irrespective of the magnitudes of the Hamiltonian parameters. If we take as typical parameters: $t=0.1$ eV, $\Delta=1$ eV, and $U_d=U_s=5$ eV, we find $J_{AF}\approx -2.3$ K from Eq. (11), which is about the same order of magnitude as the experimental value of -1K[1] (see Fig. 7).

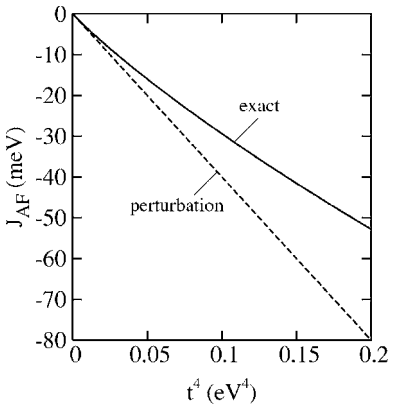

FIG. 7. Comparison of the results of the perturbation theory Eq. (11) with the exact results, obtained by the diagonalization of Eq. (6), for the intralayer exchange J_{AF}. Parameters are $U_d=U_s=5$ eV and $\Delta=1$ eV.

If the orbital ordering is different from the one shown in Fig. 6, which might occur in $LiNiO_2$, the hopping integral between Ni(1) and Na will be different from that between Ni(2) and Na. Taking them as t and t', respectively, the above expression for J_{AF} becomes modified to

$$J_{AF} = -\frac{4t^2t'^2}{\Delta^2}\left(\frac{1}{U_d} + \frac{2}{U_s + 2\Delta}\right). \quad (12)$$

For the orbital orientation shown in Fig. 8, Harrison's scaling gives us $t=V_{sd\sigma}$ and $t'=-t/2$, so that J_{AF} is reduced by a factor of 4.

IV. EFFECT OF ELECTRON-PHONON COUPLING ON MAGNETISM

A. The electron-phonon Hamiltonian

Since one of the differences between $NaNiO_2$ and $LiNiO_2$ is the atomic mass of the intervening alkali atom (Na or Li) through which the interlayer superexchange is mediated, we examine the effect of this mass on the magnetic exchange. To

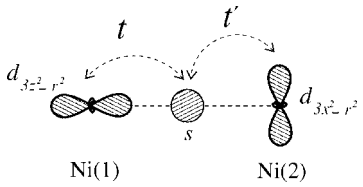

FIG. 8. Model for intersite superexchange with orbital ordering different from the ordering for $NaNiO_2$.

this end, we introduce a model electron-phonon Hamiltonian starting from a simple physical picture of the interlayer electron hopping and the resulting NiO_6 distortions as indicated in Fig. 9. The total Hamiltonian is now

$$H = H_{el} + H_{e\text{-}ph}, \tag{13}$$

where the electronic part of the Hamiltonian H_{el} is given by Eq. (5) and the electron-phonon coupling part $H_{e\text{-}ph}$ is developed below.

For the $H_{e\text{-}ph}$ part, consider the following argument. First of all, we have the two e_g^1 electrons hopping between the three sites in our model. Now, as shown by our DFT calculations, the Ni(d) orbitals have a nominal valence of $t_{2g}^6 e_g^1$ such that the Ni ion is in a low-spin configuration with a half-filled e_g orbital. When the e_g electron hops from the Ni site, the JT distortion of the NiO_6 octahedron is relaxed—Ni is t_{2g}^6 now with no degeneracy to produce the JT distortion—causing a displacement of the intermediate Na ion. For example, if the Ni(2)(e_g) and Na(s) sites are both occupied by an electron each, the NiO_6 octahedron on the Ni(1) site will be undistorted, causing a net displacement of the Na ion to the left as shown in Fig. 9. The different electronic occupations of the Ni-Na-Ni complex will give rise to different distortions as shown in Table I. For instance, if $n_1=0$, $n_2=1$, and $n_3=1$, we have an equilibrium displacement of $-\delta$ for the Na ion. As seen from the table, the equilibrium position of the Na atom for all possible electron configurations is given by the simple expression

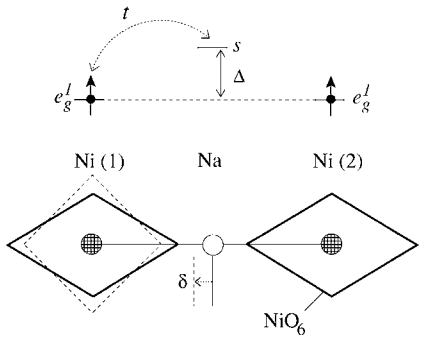

FIG. 9. Fluctuating Jahn-Teller distortion of the NiO_6 octahedra and the consequent displacement of the Na ion. The dashed square around Ni (1) indicates the undistorted NiO_6 octahedron when the e_g orbital on that site is empty, while the solid squares indicate the Jahn-Teller distorted octahedra when the Ni atoms are occupied by one e_g electron each. The fluctuating distortions of the NiO_6 octahedra in turn induce the motion of the intermediate sodium atom, which is modeled by the electron-phonon Hamiltonian $H_{e\text{-}ph}$ as discussed in the text.

TABLE I. Dependence of the equilibrium position x_0 of the sodium atom on the electronic occupations of the Ni(1), Na, and the Ni(2) sites, denoted by n_1, n_2, and n_3, respectively. The orbitals involved are e_g for the nickels and the s orbital for sodium.

n_1	n_2	n_3	Γ	x_0
1	0	1	0	0
0	1	1	−1	$-\delta$
1	1	0	1	$+\delta$

$$x_0 = \Gamma\delta, \tag{14}$$

with

$$\Gamma = (1+n_2)(n_1-n_3)/2 \tag{15}$$

and n_1, n_2, and n_3 being, respectively, the electron occupations of the Ni(1), Na, and the Ni(2) sites.

This leads to a coupling of the ionic motion to the electronic degrees of freedom, which we describe by the displaced harmonic oscillator

$$H_{e\text{-}ph}^{(1)} = \frac{p^2}{2m} + \frac{K}{2}(x-x_0)^2, \tag{16}$$

where the mass of the Na atom is denoted by m, $K=m\omega^2$ is the lattice spring constant, and ω is the frequency of the phonon mode.

There is a second part to the coupling as a result of the dependence of the electronic hopping on the distance between the atoms, which was the main ingredient of the Su-Schrieffer-Heeger model[22] of the soliton. The hopping between Ni(1) and Na is a function of the distance between the two atoms and can be approximated by keeping the linear term, so that

$$t_{12} = t(|x_{Ni_1} - x_{Na}|) \approx t - t'x, \tag{17}$$

where t is the hopping with Na fixed at the center ($x=0$) between Ni(1) and Ni(2) and x is the deviation of the Na atom from this position. Similarly, hopping between Ni(2) and Na is

$$t_{23} = t(|x_{Ni_2} - x_{Na}|) \approx t + t'x. \tag{18}$$

The constant term in hopping reproduces the electronic part H_{el} [Eq. (5)], while the linear term adds the electron-phonon coupling part

$$H_{e\text{-}ph}^{(2)} = -t'x\sum_{\sigma}(c_{1\sigma}^{\dagger}c_{2\sigma} - c_{2\sigma}^{\dagger}c_{3\sigma}) + \text{h.c.} \tag{19}$$

The total Hamiltonian now reads

$$H = H_{el} + H_{e\text{-}ph}^{(1)} + H_{e\text{-}ph}^{(2)}, \tag{20}$$

where H_{el} is given by Eq. (5) and the electron-phonon coupling parts in the second-quantized form, read

$$H_{e\text{-}ph}^{(1)} = (b^{\dagger}b + 1/2)\hbar\omega - \lambda\Gamma(b+b^{\dagger}) + (\hbar\omega)^{-1}\lambda^2\Gamma^2$$

$$H_{e\text{-}ph}^{(2)} = -\eta(b^\dagger + b)\left(\sum_\sigma (c_{1\sigma}^\dagger c_{2\sigma} - c_{2\sigma}^\dagger c_{3\sigma}) + \text{h.c.}\right), \quad (21)$$

where $b^\dagger(b)$ is the phonon creation (annihilation) operator and λ and η define the electron-phonon coupling strengths, $\lambda = (\hbar\omega\epsilon)^{1/2}$ with $\epsilon = K\delta^2/2$ and $\eta = t'[\hbar\omega/(2K)]^{1/2}$. The main parameters that determine $H_{e\text{-}ph}$ are the energy ratio $t/\hbar\omega$ and the dimensionless coupling strengths $\lambda/\hbar\omega$ and $\eta/\hbar\omega$, as may be seen by scaling the Hamiltonians Eqs. (5) and (21) by $\hbar\omega$.

To make a rough order of magnitude estimate of the coupling strengths, we take the force constant $K \sim 10$ eV/Å^2, which yields $\hbar\omega \approx 13$ meV and taking the displacement $\delta \approx 0.1$ Å from the measured oxygen displacement for the NiO_6 octahedron, we find $\lambda \sim 45$ meV, so that the dimensionless coupling parameter $\lambda/\hbar\omega \sim 3$. Similarly, with $t \approx 0.1$ eV and using Harrison scaling[18] for t', so that $t' \approx 0.2$ eV/Å, which yields $\eta \sim 10$ meV or $\lambda/\hbar\omega \sim 1$.

Note that in our model, we have not kept the vibrations of the oxygen octahedra, which of course must be considered if one is interested in the effect of the oxygen mass. The electron-lattice coupling affects magnetism because it modifies the bare electron hopping parameters, which is the subject of study in the next section.

B. Solution of the Hamiltonian

The lattice effects may be studied either via the Lang-Firsov approach or by exact diagonalization. The former approach, although approximate, yields a physically appealing result by casting the lattice effects in terms of the renormalization of the electron hopping parameters. We treat $H_{el} + H_{e\text{-}ph}^{(1)}$ by the variational Lang-Firsov (VLF) approach for the sake of illustration, while the full Hamiltonian is solved by exact diagonalization.

Within the VLF approach,[23–25] which is a variational method based on the canonical Lang-Firsov transformation,[26] we introduce the unitary transformation of the Hamiltonian H'

$$\tilde{H} = e^{-S} H' e^{S},$$

$$S = \alpha \frac{\lambda}{\hbar\omega}\Gamma(b^\dagger - b), \quad (22)$$

where α is a variational parameter and S is anti-Hermitian, so that the transformation described by $U = e^{-S}$ is unitary and $H' = H_{el} + H_{e\text{-}ph}^{(1)}$. Note that the transformation can diagonalize the electron-phonon part of the Hamiltonian exactly with the choice of $\alpha = -1$ [see Eqs. (25) and (26)], but the electronic part becomes modified, with the phonon operators entering the electronic Hamiltonian Eq. (25). The variational parameter α is a measure of the phonon "dressing" of the electron, the so-called Lang-Firsov small polaron.

Although the transformation is designed to work well in the strong coupling limit, we find that it works quite well in our case, where the coupling $\lambda/\hbar\omega$ is not that high. A better but more involved Lang-Firsov transformation[23,24] consists of three consecutive variational transformations defined by S, $S' = \beta(b^\dagger - b)$, and $S'' = \gamma(b^\dagger b^\dagger - bb)$, where α, β, and γ are variational parameters, each designed to work well in the high, low, and intermediate coupling regimes respectively.

Using the general expression for a transformed operator in terms of the corresponding commutators

$$\tilde{A} = e^{-S} A e^{S} = A + [A,S] + \frac{1}{2!}[[A,S],S] + \cdots, \quad (23)$$

the transformed creation operators can be shown to be

$$\tilde{b}^\dagger = b^\dagger - \alpha(\lambda/\hbar\omega)\Gamma,$$

$$\tilde{c}_i^\dagger = e^{-B_i} c_i^\dagger, \quad (24)$$

where

$$B_i = \frac{\alpha\lambda}{2\hbar\omega}(b^\dagger - b)[\delta_{2i}(n_1 - n_3) + (1 + n_2)(\delta_{1i} - \delta_{3i})].$$

The transformed Hamiltonians read

$$\tilde{H}_{el} = t\sum_{\langle ij\rangle\sigma} c_{i\sigma}^\dagger e^{(\alpha\lambda)/(2\hbar\omega)\nu_{ij}(b^\dagger - b)} c_{j\sigma} + \text{h.c.} + \sum_i (\varepsilon_i n_i + U_i n_{i\uparrow} n_{i\downarrow}) \quad (25)$$

and

$$\tilde{H}_{e\text{-}ph} = \hbar\omega\left(b^\dagger b + \frac{1}{2}\right) - (1 + \alpha)\lambda\Gamma(b + b^\dagger) + (1 + \alpha)^2 \frac{\lambda^2}{\hbar\omega}\Gamma^2, \quad (26)$$

where $\nu_{ij} = -\nu_{ji}$, $\nu_{12} = (3/2) - n_1$, and $\nu_{23} = (3/2) - n_3$. The Hamiltonian is then averaged over the bare phonon vacuum $|\Psi_{ph}^0\rangle$, which yields

$$\bar{H} \approx \langle\Psi_{ph}^0|\tilde{H}|\Psi_{ph}^0\rangle = t\sum_{\langle ij\rangle\sigma} c_{i\sigma}^\dagger \exp\left(-\frac{\alpha^2\lambda^2}{8\hbar^2\omega^2}\nu_{ij}^2\right) c_{j\sigma} + \text{h.c.}$$
$$+ \sum_i (\varepsilon_i n_i + U_i n_{i\uparrow} n_{i\downarrow}) + \frac{\hbar\omega}{2} + (1 + \alpha)^2 \frac{\lambda^2}{\hbar\omega}\Gamma^2. \quad (27)$$

Note that as compared to the original electronic Hamiltonian H_{el}, the hopping parameter becomes renormalized to a lower value, which is readily seen to reduce the magnetic exchange from the fourth-order perturbation theory. Also, $\bar{H}$ will clearly yield a variational upper bound to the ground-state energy, since the Hilbert space is now restricted to the zero-phonon subspace only.

In the exact diagonalization, the ground-state wave function is simply expanded in the joint electron-phonon occupation-number basis set: $|G\rangle = \Sigma_i a_i |i\rangle$, and the resulting Hamiltonian matrix is diagonalized using the Lanczos method. The Hamiltonian is truncated by keeping only a finite number of phonons, making sure that convergence of the ground-state energy has been achieved as a function of the number of phonons. Typically, 10 to 50 phonons are needed to achieve convergence.

Figure 10 shows the calculated energies using three different methods. The results indicate that the Lang-Firsov Hamiltonian is quite accurate as far as the ground-state energy is concerned. Within the VLF approximation, the

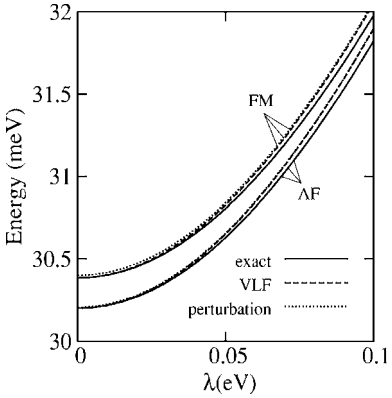

FIG. 10. Energy of the FM and AF states using three different methods: (a) Exact diagonalization of the full, untransformed Hamiltonian Eq. (13); (b) Exact diagonalization of the Lang-Firsov Hamiltonian $\bar{H}$ [Eq. (27); and (c)] The fourth-order perturbation theory on the Lang-Firsov Hamiltonian $\bar{H}$. Note that the VLF energy is always above the exact energy, forming a variational lower bound to the ground-state energy. Parameters used here are $\hbar\omega$=100 meV, t=0.1 eV, U_d=5 eV, U_s=5 eV, and Δ=1 eV. The quadratic dependence of energy on λ is understood in terms of the last term of the Lang-Firsov Hamiltonian Eq. (27).

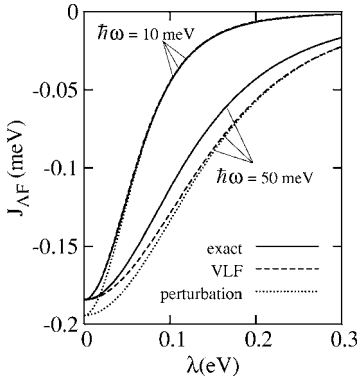

FIG. 11. Plot of the exchange interaction J_{AF} as a function of the electron-phonon coupling strength λ, with η=0. J_{AF} remains always antiferromagnetic, but its magnitude is decreased with increased strength λ of the electron-phonon coupling. Parameters used are the same as the previous figure except for $\hbar\omega$.

ground-state energies for the FM and AF configurations are obtained by diagonalizing the Hamiltonian Eq. (27) and then by minimizing the energy as a function of the variational parameters α. In general this method would give a different minimum value of α for the FM and the AF configurations, but in practice we find that the minimum in α for the FM and AF configuration are very close $\alpha_{AF} \approx \alpha_{FM} \sim 0.01$, so that we take them to be the same in writing down the perturbative result in Eq. (28) below.

Such a small value of α is indicative of the fact that the electron-phonon coupling does not affect the electronic system strongly. Indeed, as seen from the renormalized operators, Eq. (24), if α is zero, then we have just the bare electrons and phonons.

The Lang-Firsov Hamiltonian (27) may be written in a matrix form similar to Eq. (6) with modified off-diagonal hopping elements. Fourth-order perturbation theory carried out following the procedure of Sec. III B yields in the present case the following result for the interlayer exchange:

$$J_{AF} \approx \frac{-4t^4 e^{-5\alpha^2\epsilon/(2\hbar\omega)}}{(\Delta+\epsilon)^2} \times \left[\frac{2e^{-2\alpha^2\epsilon/\hbar\omega}}{U_s+2\Delta} + \frac{1}{U_d+\epsilon}\right], \quad (28)$$

where $\epsilon=\lambda^2/\hbar\omega$ as defined before. In the limit of no electron-phonon coupling, $\lambda/\hbar\omega \to 0$, this expression clearly reduces to Eq. (11). As indicated from the expression, the exchange remains always antiferromagnetic, however, the electron-phonon coupling diminishes the magnitude of J_{AF}. The result of the perturbation expression Eq. (28) together with the exact diagonalization and the Lang-Firsov results have been shown in Fig. 11.

The second part of the coupling $H^{(2)}_{e\text{-}ph}$ is somewhat cumbersome to treat by the Lang-Firsov approach, since it contains off-diagonal hopping terms. However, this coupling, parametrized by the strength η, also reduces the magnetic exchange, as seen from Fig. 12, obtained from exact diagonalization.

We now turn to the question of the dependence of the exchange interaction on the mass of the alkali atom. We have computed this by diagonalizing the full Hamiltonian, keeping all couplings. As mass is varied, the phonon frequency $\hbar\omega$ as well as the coupling strengths λ and η change, which are calculated using the parameters given in the caption of Fig. 13. The figure shows the result for two different values for the Ni to Na charge-transfer energy Δ. Although the measured $J_{AF} \approx -1$ K is already quite small for $NaNiO_2$, we find a reduction of J_{AF} by only a small amount in going from ^{23}Na to ^{7}Li. We thus conclude that the difference in mass alone can not describe the differences in the magnetic behavior between the two compounds $NaNiO_2$ and $LiNiO_2$.

A further reduction in J_{AF} could come from changes in the electronic structure in going from $NaNiO_2$ to $LiNiO_2$. For example, neutron scattering experiments[14] have shown that unlike $NaNiO_2$, no long-range orbital ordering exists in $LiNiO_2$. An orbital ordering different from $NaNiO_2$ would diminish J_{AF} as indicated in the last part of Sec. III B.

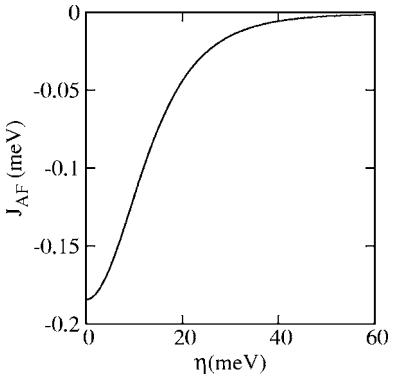

FIG. 12. Plot of the exchange interaction J_{AF} as a function of the electron-phonon coupling strength η, with λ=0, obtained from diagonalization of the full Hamiltonian Eq. (20). Parameters are $\hbar\omega$=10 meV, t=0.1 eV, U_d=5 eV, U_s=5 eV, and Δ=1 eV.

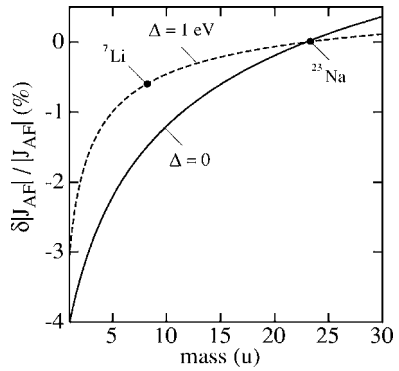

FIG. 13. Dependence of the magnitude of the interplanar exchange J_{AF} on the mass of the alkali atom for the parameters: $K=10$ eV/Å^2, $t=0.1$ eV, $t'=0.2$ eV/Å, $U_d=5$ eV, and $U_s=5$ eV. Δ is the Ni to Na charge transfer energy and $\delta|J_{AF}|/|J_{AF}| \equiv [|J_{AF}(m)|-|J_{AF}(Na)|]\times|J_{AF}(Na)|^{-1}$. A larger Δ suppresses exchange by inhibiting electron transfer between Ni(1) and Ni(2).

V. CONCLUSION

We have studied the electronic structure and the exchange interaction in the nickelate compound $NaNiO_2$. The density-functional results showed a ferrodistorsive orbital ordering with all Ni(e_g) orbitals in the crystal pointed along the Ni-O-Na direction, i.e., along the same crystallographic direction.

Both the intra- and the interlayer exchange interactions are weak because of different reasons. The intralayer exchange is mediated via the 90° Ni-O-Ni superexchange and is weakly ferromagnetic, consistent with the Goodenough-Kanamori-Anderson rules, while the interlayer exchange is even weaker and antiferromagnetic due to the long Ni-O-Na-O-Ni superexchange path.

Finally, we studied the effect of the electron-phonon coupling on the magnetic exchange by solving a simple model Hamiltonian from exact diagonalization, variational Lang-Firsov, and perturbation theoretic approaches. While we found that the interlayer exchange is indeed diminished by coupling to the lattice, this effect alone is not large enough to alter the magnetic behavior in going from $NaNiO_2$ to $LiNiO_2$. What is happening is that the interlayer superexchange, which is especially small in this class of compounds owing to the long Ni-O-Na-O-Ni superexchange path, becomes enhanced in $NaNiO_2$ due to orbital ordering (Ni orbitals pointed along Ni-O facilitating electron hopping, which in turn enhances the magnetic exchange). The J_{AF} (measured value ~1K), although still relatively weak, is nevertheless strong enough to support magnetism between the layers and hence in the entire three-dimensional (3D) structure. Within this scenario, what is suggested is that the weak magnetism in $NaNiO_2$ is the result of the specific type of orbital ordering in the compound, which allows for a strong enough exchange between the planes.

ACKNOWLEDGMENT

We acknowledge support of this work by the U. S. Department of Energy through Grant No. DE-FG02-00ER45818.

[1] E. Chappel, M. Núñez-Regueiro, G. Chouteau, O. Isnard, and C. Darie, Eur. Phys. J. B **17**, 615 (2000).
[2] D. Mermin and H. Wagner, Phys. Rev. Lett. **17**, 1133 (1966); P. C. Hohenberg, Phys. Rev. **158**, 383 (1967).
[3] E. Terukov, W. Reichelt, D. Ihle, and H. Oppermann, Phys. Status Solidi B **95**, 491 (1979).
[4] J. P. Franck, I. Isaac, W. Chen, J. Chrzanowski, and J. C. Irwin, Phys. Rev. B **58**, 5189 (1998).
[5] I. Isaac and J. P. Franck, Phys. Rev. B **57**, R5602 (1998).
[6] G. M. Zhao, K. Conder, and K. A. Mller, Nature (London) **381**, 676 (1996).
[7] E. Chappel, M. Núñez-Regueiro, F. Dupont, G. Chouteau, C. Darie, and A. Sulpice, Eur. Phys. J. B **17**, 609 (2000).
[8] H. Meskine and S. Satpathy, J. Appl. Phys. **97**, 10A314 (2005).
[9] O. K. Andersen and O. Jepsen, Phys. Rev. Lett. **53**, 2571 (1984).
[10] O. K. Andersen, Phys. Rev. B **12**, 3060 (1975).
[11] V. I. Anisimov, F. Aryasetiawan, and A. I. Lichtenstein, J. Phys.: Condens. Matter **9**, 767 (1997).
[12] U. von Barth and L. Hedin, J. Phys. C **5**, 1629 (1972).
[13] L. D. Dyer, B. S. Borie, G. P. Smith, J. Am. Chem. Soc. **76**, 1499 (1954).
[14] J. H. Chung, Th. Proffen, S. Shamoto, A. M. G. Jhorayeb, L. Croguennec, W. Tian, B. C. Seles, R. Jin, D. Mandrus, and T. Egami, Phys. Rev. B **71**, 064410 (2005).
[15] J. B. Goodenough, *Magnetism and the Chemical Bond* (Interscience, New York, 1963).
[16] D. Khomskii in *Spin Electronics*, edited by M. Ziese and M. J. Thornton (Springer, Berlin, 2000).
[17] R. D. Mattuck, *Guide to Feynman Diagrams in the Many-Body Problem* (Dover, New York, 1992), p. 112.
[18] W. A. Harrison, *Electronic Structure and the Properties of Solids* (Freeman, San Francisco, 1980).
[19] M. V. Mostovoy and D. I. Khomskii, Phys. Rev. Lett. **89**, 227203 (2002).
[20] L. D. Landau and E. M. Lifshitz, *Quantum Mechanics* (Butterworth-Heinemann, Oxford, 1977).
[21] The expression Eq. 11 for the interlayer exchange corrects the misprint in Eq. 4 in our earlier paper (Ref. 8), where a factor of 2 is missing.
[22] W. P. Su, J. R. Schrieffer, and A. J. Heeger, Phys. Rev. Lett. **42**, 1698 (1979).
[23] H. Fehske, H. Röder, G. Wellein and, and A. Mistriotis, Phys. Rev. B **51**, 16582 (1995).
[24] H. Röder, J. Zang, and A. R. Bishop, Phys. Rev. Lett. **76**, 1356 (1996).
[25] G. Wellein and H. Fehske, Phys. Rev. B **58**, 6208 (1998).
[26] L. G. Lang and Y. A. Firsov, Sov. Phys. JETP **16**, 1301 (1963).